International Journal of Control

ISSN: 0020-7179 (Print) 1366-5820 (Online) Journal homepage: http://www.tandfonline.com/loi/tcon20

Intrinsic dynamics and total energy-shaping control of the ballbot system

A. C. Satici, A. Donaire & B. Siciliano

To cite this article: A. C. Satici, A. Donaire & B. Siciliano (2016): Intrinsic dynamics and total energy-shaping control of the ballbot system, International Journal of Control, DOI: 10.1080/00207179.2016.1264630

To link to this article: http://dx.doi.org/10.1080/00207179.2016.1264630

Accepted author version posted online: 23 Nov 2016.
Published online: 08 Dec 2016.

INTERNATIONAL JOURNAL OF CONTROL, 2016
http://dx.doi.org/10.1080/00207179.2016.1264630

Taylor & Francis
Taylor & Francis Group

Intrinsic dynamics and total energy-shaping control of the ballbot system

A. C. Satici[a], A. Donaire[b] and B. Siciliano[b]

[a]Electrical Engineering and Computer Science, Massachusetts Institute of Technology, Cambridge, MA, USA; [b]Ingegneria Elettrica e Tecnologie dell'Informazione, Università degli Studi di Napoli Federico II, Naples, Italy

ABSTRACT

Research on bipedal locomotion has shown that a dynamic walking gait is energetically more efficient than a statically stable one. Analogously, even though statically stable multi-wheeled robots are easier to control, they are energetically less efficient and have low accelerations to avoid tipping over. In contrast, the ballbot is an underactuated, nonholonomically constrained mobile robot, whose upward equilibrium point has to be stabilised by active control. In this work, we derive coordinate-invariant, reduced, Euler–Poincaré equations of motion for the ballbot. By means of partial feedback linearisation, we obtain two independent passive outputs with corresponding storage functions and utilise these to come up with energy-shaping control laws which move the system along the trajectories of a new Lagrangian system whose desired equilibrium point is asymptotically stable by construction. The basin of attraction of this controller is shown to be almost global under certain conditions on the design of the mechanism which are reflected directly in the mass matrix of the unforced equations of motion.

ARTICLE HISTORY
Received 9 May 2016
Accepted 20 November 2016

KEYWORDS
Euler–Poincaré equations; energy shaping; passivity; underactuated robotics; reduction of dynamics

1. Introduction

Contemporary research on robotics has steered towards the incorporation of robots into everyday lives of humans. Robots are expected to safely interact with humans both outdoors and in human environments. This motivation requires robots not only to be mobile and slim but also tall enough to facilitate interaction. On the other hand, conventional multi-wheeled statically stable robots are typically built to have a low centre of gravity in order to prevent them from easily tipping over. The satisfaction of these two conflicting requirements urges the mobile robots to have large, wide, and heavy bases. At the cost of the necessity to design a more complicated controller, a more efficient method to tackle the interaction problem is to utilise dynamically stable robots.

One of the most popular dynamically balancing robots is the two-wheeled Segway (Nguyen et al., 2004). The ballbot was introduced as a mobile robot moving on a single spherical omnidirectional wheel (Lauwers, Kantor, & Hollis, 2005, 2006). The ballbot, whose design is detailed in Nagarajan, Kantor, and Hollis (2013) and Nagarajan, Mampetta, Kantor, and Hollis (2009) is typically slim and as tall as an adult human, rendering it able to interact with humans while navigating constrained environments.

Even though a variant of this robot has been built by many laboratories (Hertig, Schindler, Bloesch, Remy, & Siegwart, 2013; Leutenegger & Fankhauser, 2010), its control framework has been restricted to the use of classic methods such as linearisation about a desired equilibrium in coordinates and proportional-integral-derivative (PID) controllers (Kumaga & Ochiai, 2009; Leutenegger & Fankhauser, 2010). Derivation of the equations of motion of the ballbot with a 3-DoF manipulator mounted on top using both Lagrange's and Kane's methods have been performed in Asgari, Zarafshan, and Moosavian (2015). The authors have confirmed that the two approaches agree with each other with a numerical simulation. They have also designed two control laws for the x–y motion of the ballbot and for manipulation, respectively, without explicitly addressing stability properties. Moreover, many controllers are typically developed by restricting the dynamics of the ballbot to a vertical 2D plane and applied to the 3D robot by an ad hoc extension to two distinct vertical planes. This procedure inevitably ignores the energetic interaction of the full dynamics of the robot along these planes. Trajectory planning based on motion primitives has been presented in Nagarajan, Kantor, and Hollis (2012), while in Nagarajan, Kim, and Hollis (2012), authors plan a trajectory for the ballbot equipped with the right and left arms. A sliding-mode controller has also been designed for this system in Liao, Tsai, Li, and Chan (2008). For the most part, the equations of motion of the full dynamics of the ballbot have been derived in coordinates, which injects a fair bit of

CONTACT A. C. Satici acsatici@mit.edu

unnecessary complexity into the problem formulation, requires the use of a symbolic manipulation software and a decent amount of storage space in the computer (Leutenegger & Fankhauser, 2010). The only exception to this trend has been provided in Inal, Morgul, and Saranli (2012), where the authors derive a dynamic model of the ballbot which additionally assumes that the body has no yaw motion relative to the ball using Newton's laws. This lengthy procedure, which was omitted from the paper due to space considerations, leads to a dynamical model of the system which is not particularly easy to work with for control synthesis. Finally, in Larimi, Zarafshan, and Moosavian (2015), a stabilisation algorithm for a two-wheeled mobile manipulator (TWMM), which is a robot with similar characteristics with the ballbot, has been presented. The controller designed in this paper utilises the zero moment point (ZMP) idea from the bipedal robotic literature to asymptotically stabilise the motion of the TWMM.

In this paper, we derive the Euler–Lagrange equations of motion of the full dynamics of the ballbot without resort to any coordinate system. This yields a compact, yet explicit representation of the equations of motion, which recover the 2D dynamics of the ballbot, restricted to a vertical plane, given in the literature (Nagarajan et al., 2013). Preliminary results on the derivation and linearisation of the intrinsic dynamics of the ballbot is reported in Satici, Ruggiero, Lippiello, and Siciliano (2016). The Euler–Poincaré dynamics developed in this paper yields a reduced set of 10 first-order ordinary differential equations (ODEs) that govern the motion of the ballbot as opposed to the conventional Newton–Euler approach which would yield 16 first-order ODEs. We develop energy-shaping control laws, that use the available control inputs to make the system look like a new Lagrangian system with a desired asymptotically stable equilibrium point, for both the 2D and the 3D dynamics of the ballbot. While in the 2D case, we are able to follow the procedure outlined in Donaire et al. (2016) so as to shape the energy, for the 3D-case, this procedure needs to be extended because the form of the Euler–Poincaré does not exactly match the form of the Euler–Lagrange equations as handled in that work. The derivation of the total energy-shaping control law for the ballbot shows the applicability of the approach to a system with considerably more number of states than the examples previously reported in the literature. The main contribution of this paper is providing an intrinsic and unified framework to study the dynamics and control of the balancing system consisting of a heavy top on a spherical wheel as well as providing nonlinear energy-shaping control law whose basin of attraction is almost global as long as the mechanism is judiciously designed.

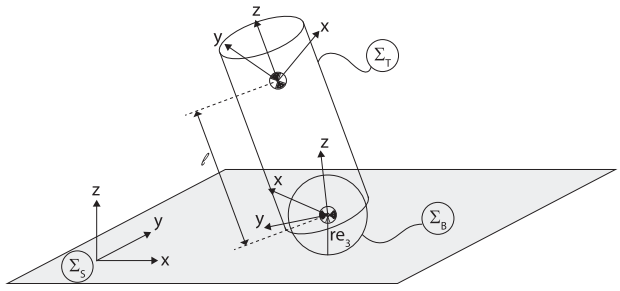

Figure 1. Ballbot: bodies and frames.

2. Lagrangian dynamics of the ballbot

In this section, we present the background information to be used in the remainder of this paper including the kinematics and dynamics of the ballbot. We start by noting that every vector quantity in this paper is represented in the spatial frame.

2.1 Background and kinematics

The skeleton diagram of the ballbot is depicted in Figure 1. It is constructed via the interconnection of a rigid spherical wheel and a rigid cylindrical body such that the body is unable to translate with respect to the ball but is free to move otherwise. Therefore, the configuration manifold of the ballbot is $Q = \mathbb{R}^2 \times SO(3) \times SO(3)$. The inertial frame, denoted by Σ_S, is fixed to a horizontal plane. The spherical wheel is represented by the frame Σ_B and is assumed to have its centre of mass at its geometric centre. As a result, the vector from the point of contact of the sphere with the ground and its centre of mass is given by re_3 in the inertial frame. Here, r denotes the radius of the sphere, and throughout the paper, e_n denotes the nth standard unit vector. The cylindrical rigid body situated on the wheel is referred to as the 'top' and is bestown a reference frame denoted by Σ_T. The centre of mass of the top is assumed to lie on the central axis of its geometrical shape at a distance $l > 0$ from the centre of the ball. The ball is assumed to roll without slipping, yielding the well-known nonholonomic constraint between the time derivative of its position vector p_{sb} and its spatial angular velocity ω_{sb}

$$\dot{p}_{sb} = r\omega_{sb} \times e_3 = r\hat{\omega}_{sb}e_3, \tag{1}$$

where we introduced the *hat* $\wedge$ operator, which stands for the standard isomorphism between $\mathbb{R}^3$ and $\mathfrak{so}(3)$. Its inverse is denoted by the symbol $\vee$, known as the *vee* map (Murray, Sastry, & Zexiang, 1994).

The kinematics of the orientation of the ball and the top are given in the spatial frame by the familiar rigid

body orientation kinematics

$$\dot{R}_{sb} = \hat{\omega}_{sb} R_{sb}, \quad \dot{R}_{st} = \hat{\omega}_{st} R_{st}. \tag{2}$$

Using notation and methods from Murray et al. (1994), we express the velocity of the top with respect to the inertial frame V_{st} in terms of the velocity of the ball with respect to the inertial frame V_{sb} and the velocity of the top with respect to the ball V_{bt}

$$V_{st} = \begin{bmatrix} v_{st} \\ omega_{st} \end{bmatrix} = \begin{bmatrix} v_{sb} + p_{sb} \times R_{sb}\omega_{bt} \\ omega_{sb} + R_{sb}\omega_{bt} \end{bmatrix}. \tag{3}$$

We can now compute the time derivative of p_{st} as a function of the time derivative of p_{sb}, the angular velocity of the top with respect to the inertial frame and the orientation of the top:

$$\dot{p}_{st} = \dot{p}_{sb} + l\omega_{st} \times R_{st} e_3. \tag{4}$$

Throughout this paper, the dot product of two vectors is denoted by $x \cdot y = x^T y$ for any $x, y \in \mathbb{R}^n$. Unless it is conspicuous from the context, the $n \times n$ identity matrix is denoted by I_n. Similarly, the $n \times m$ matrix composed of zero elements is denoted by $0_{n\times m}$, and it is written as 0_n if $n = m$. Some properties of the hat map that we freely use in the remainder are as follows:

$$\begin{aligned} \hat{x}y = x \times y = -y \times x = -\hat{y}x, \\ x \cdot \hat{y}z = y \cdot \hat{z}x = z \cdot \hat{x}y, \\ hat{x}\hat{y}\hat{z} = (x \cdot z)\, y - \left(x \cdot y\right) z, \end{aligned}$$

for any $x, y, z \in \mathbb{R}^3$.

2.2 Lagrangian

We write the Lagrangian of the ballbot in the spatial frame, that is, as seen by an observer stationary in the inertial frame. Note that it is imperative that the rolling constraint (1) not be inserted into the Lagrangian before its variation is taken. If the variation of the Lagrangian is taken after the substitution of the nonholonomic constraints, this yields the vakonomic equations, which are known to disagree with the dynamics of rigid bodies. Instead, one should take the variation before the imposition of the nonholonomic constraints, leading to the Lagrange–d'Alembert equations, the correct equations of motion (Baillieul, Bloch, Crouch, & Marsden, 2008; Lewis & Murray, 1995). The inertia of the ball and the top expressed in the inertial frame I_b, $I_t \in \mathrm{Sym}^2(Q)$, respectively, are positive-definite symmetric (0, 2)-tensor fields on Q. Their respective masses are denoted by m_b and m_t.

The kinetic energy of the ball is given by the sum of its rotational and translational kinetic energies, while its potential energy is zero, since its height with respect to the inertial frame remains a constant

$$\begin{aligned} K_b &= \frac{1}{2}\omega_{sb} \cdot I_b \omega_{sb} + \frac{1}{2} m_b \dot{p}_{sb} \cdot \dot{p}_{sb}, \\ V_b &= 0. \end{aligned}$$

The potential energy of the top is given by the height of its centre of mass from the horizontal multiplied by its mass. The kinetic energy of the top can be written in terms of the rotational velocity of the top and the translational velocity of the ball with respect to the inertial frame by substituting from (4):

$$\begin{aligned} K_t &= \frac{1}{2}\omega_{st} \cdot I_t \omega_{st} + \frac{1}{2} m_t \dot{p}_{st} \cdot \dot{p}_{st} \\ &= \frac{1}{2}\omega_{st} \cdot I_t \omega_{st} + \frac{1}{2} m_t l^2 \omega_{st} \cdot \omega_{st} + \frac{1}{2} m_t \dot{p}_{sb} \cdot \dot{p}_{sb} \\ &\quad - \frac{1}{2} m_t l^2 \left(\omega_{st} \cdot R_{st} e_3\right)^2 + m_t l \dot{p}_{sb} \cdot \left(\omega_{st} \times R_{st} e_3\right), \\ V_t &= m_t g l e_3 \cdot R_{st} e_3. \end{aligned}$$

Therefore, the Lagrangian $L = K - V = K_t + K_b - V_t$ is

$$\begin{aligned} L = &\frac{1}{2}\omega_{st} \cdot I_t \omega_{st} + \frac{1}{2} m_t l^2 \omega_{st} \cdot \omega_{st} + \frac{1}{2}\omega_{sb} \cdot I_b \omega_{sb} \\ &+ \frac{1}{2}(m_b + m_t)\, \dot{p}_{sb} \cdot \dot{p}_{sb} - \frac{1}{2} m_t l^2 \left(\omega_{st} \cdot R_{st} e_3\right)^2 \\ &+ m_t l \dot{p}_{sb} \cdot \left(\omega_{st} \times R_{st} e_3\right) - m_t g l e_3 \cdot R_{st} e_3. \end{aligned} \tag{5}$$

Let us define an element of the unit 2-sphere $\Gamma := R_{st} e_3$. This quantity represents the direction of the centre of mass of the top expressed in the inertial coordinates. Next, we write the Lagrangian in terms of Γ, the angular velocity of the top with respect to the inertial frame and the angular velocity of the ball with respect to the top, all expressed in the inertial frame. We represent the latter quantity by $\bar{\omega}_{tb}$ and compute it by $\bar{\omega}_{tb} = \omega_{sb} - \omega_{st}$. When the Lagrangian (5) is expressed with these quantities, it takes the reduced form

$$\begin{aligned} \ell = &\frac{1}{2}\left\langle \omega_{st}, \left(I_t + I_b + m_t l^2 I_3\right) \omega_{st} \right\rangle + \left\langle \omega_{st}, I_b \bar{\omega}_{tb} \right\rangle \\ &+ \frac{1}{2}\left\langle \bar{\omega}_{tb}, I_b \bar{\omega}_{tb} \right\rangle + \frac{1}{2}(m_b + m_t)\left\langle \dot{p}_{sb}, \dot{p}_{sb} \right\rangle \\ &- \frac{1}{2} m_t l^2 \left\langle \omega_{st}, \Gamma \right\rangle^2 + m_t l \left\langle \dot{p}_{sb}, \omega_{st} \times \Gamma \right\rangle - m_t g l \left\langle e_3, \Gamma \right\rangle. \end{aligned} \tag{6}$$

2.3 Euler–Poincaré equations of the ballbot

The equations of motion of the ballbot can be reduced from TQ to $\mathfrak{so}(3) \times \mathfrak{so}(3) \times \mathbb{S}^2 \times \mathbb{R}^2$ to yield the Euler–Poincaré equations (Schneider, 2002) for the ballbot. We can derive the evolution of Γ by differentiating its definition and using the kinematics of the rigid body,

$$\dot{\Gamma} = \dot{R}_{st} e_3 = \omega_{st} \times R_{st} e_3 = \omega_{st} \times \Gamma, \tag{7a}$$

$$\dot{\Gamma} + \Gamma \times \omega_{st} = 0. \tag{7b}$$

We freely make use of the following identities when taking the variation of the reduced Lagrangian (6):,

$$\delta R^{-1} = -R^{-1} \delta R R^{-1}, \tag{8a}$$

$$\delta I = \delta R R^{-1} I - I \delta R R^{-1}, \tag{8b}$$

$$\delta\omega = \dot{\eta} + \eta \times \omega, \tag{8c}$$

$$\delta\dot{p} = \frac{\mathrm{d}}{\mathrm{d}t}(\delta p). \tag{8d}$$

where $R \in SO(3), \omega \in \mathfrak{so}(3), p \in \mathbb{R}^3$, and $\mathfrak{so}(3) \ni \hat{\eta} = \delta R R^{-1}$. The action integral is given by $s = \int \ell \mathrm{d}t$, whose variation, $\delta s = \int \delta\ell \mathrm{d}t$, is computed by

$$\delta s = \int \left(\frac{\delta\ell}{\delta R_{st}} \delta R_{st} + \frac{\delta\ell}{\delta\omega_{st}} \delta\omega_{st} + \frac{\delta\ell}{\delta\bar{\omega}_{tb}} \delta\bar{\omega}_{tb} + \frac{\delta\ell}{\delta\Gamma} \delta\Gamma + \frac{\delta\ell}{\delta\dot{p}_{sb}} \delta\dot{p}_{sb} \right) \mathrm{d}t.$$

Let us compute the individual terms making use of the additional relation $\delta\Gamma = \eta_{st} \times \Gamma$

$$\int \frac{\delta\ell}{\delta R_{st}} \delta R_{st} \mathrm{d}t = \int \frac{1}{2} \left\langle \omega_{st}, \left(\hat{\eta}_{st} I_t - I_t \hat{\eta}_{st} \right) \omega_{st} \right\rangle \mathrm{d}t = \int \langle I_t \omega_{st} \times \omega_{st}, \eta_{st} \rangle \, \mathrm{d}t,$$

$$\int \frac{\delta\ell}{\delta\omega_{st}} \delta\omega_{st} \mathrm{d}t = \int \left\langle \frac{\partial\ell}{\partial\omega_{st}}, \dot{\eta}_{st} + \eta_{st} \times \omega_{st} \right\rangle \mathrm{d}t = \int \left\{ \left\langle -\frac{\mathrm{d}}{\mathrm{d}t} \frac{\partial\ell}{\partial\omega_{st}} + \omega_{st} \times \frac{\partial\ell}{\partial\omega_{st}}, \eta_{st} \right\rangle \right\} \mathrm{d}t$$

$$= \int \langle - \left(\hat{\omega}_{st} I_t - I_t \hat{\omega}_{st} \right) \omega_{st} - \left(I_t + I_b + m_t l^2 I_3 \right) \dot{\omega}_{st} - I_b \dot{\bar{\omega}}_{tb} + m_t l^2 \left(\langle \dot{\omega}_{st}, \Gamma \rangle \Gamma + \langle \omega_{st}, \Gamma \rangle \omega_{st} \times \Gamma \right) - m_t l \left((\omega_{st} \times \Gamma) \times \dot{p}_{sb} + \Gamma \times \ddot{p}_{sb} \right) + \omega_{st} \times \left(I_t + I_b + m_t l^2 I_3 \right) \omega_{st} + \omega_{st} \times I_b \bar{\omega}_{tb} - m_t l^2 \langle \omega_{st}, \Gamma \rangle \omega_{st} \times \Gamma + m_t l \left(\omega_{st} \times \left(\Gamma \times \dot{p}_{sb} \right) \right), \eta_{st} \rangle \mathrm{d}t,$$

$$\int \frac{\delta\ell}{\delta\bar{\omega}_{tb}} \delta\bar{\omega}_{tb} \mathrm{d}t = \int \langle - \frac{\mathrm{d}}{\mathrm{d}t} \frac{\partial\ell}{\partial\bar{\omega}_{tb}} + \bar{\omega}_{tb} \times \frac{\partial\ell}{\partial\bar{\omega}_{tb}} \, rangle \mathrm{d}t = \int \langle - I_b \left(\dot{\omega}_{st} + \dot{\bar{\omega}}_{tb} \right) + \bar{\omega}_{tb} \times I_b \left(\omega_{st} + \bar{\omega}_{tb} \right), \bar{\eta}_{tb} \rangle \mathrm{d}t,$$

$$\int \frac{\delta\ell}{\delta\Gamma} \delta\Gamma \mathrm{d}t = \int \left\langle \frac{\partial\ell}{\partial\Gamma}, \eta_{st} \times \Gamma \right\rangle \mathrm{d}t = \int \left\langle \Gamma \times \frac{\partial\ell}{\partial\Gamma}, \eta_{st} \right\rangle \mathrm{d}t = \int \langle - m_t l^2 \langle \omega_{st}, \Gamma \rangle \Gamma \times \omega_{st} + m_t l \left(\Gamma \times \left(\dot{p}_{sb} \times \omega_{st} \right) \right) - m_t g l \Gamma \times e_3, \eta_{st} \rangle \mathrm{d}t,$$

$$\int \frac{\delta\ell}{\delta\dot{p}_{sb}} \delta\dot{p}_{sb} \mathrm{d}t = \int \left\langle - \frac{\mathrm{d}}{\mathrm{d}t} \frac{\partial\ell}{\partial\dot{p}_{sb}}, \delta p_{sb} \right\rangle \mathrm{d}t = \int \langle - (m_b + m_t) \ddot{p}_{sb} - m_t l \big(\dot{\omega}_{st} \times \Gamma + \omega_{st} \times (\omega_{st} \times \Gamma) \big), \delta p_{sb} \rangle \mathrm{d}t = \int \langle - (m_b + m_t) r \ddot{p}_{sb} - m_t l \big(\dot{\omega}_{st} \times \Gamma + \omega_{st} \times (\omega_{st} \times \Gamma) \big), (\eta_{st} + \bar{\eta}_{tb}) \times e_3 \rangle \mathrm{d}t = \int \langle - (m_b + m_t) r e_3 \times \ddot{p}_{sb} - m_t r l \big(e_3 \times (\dot{\omega}_{st} \times \Gamma) + e_3 \times (\omega_{st} \times (\omega_{st} \times \Gamma)) \big), (\eta_{st} + \bar{\eta}_{tb}) \rangle \mathrm{d}t.$$

Keeping accordance with the literature, we assume that the rotation of the ball along the inertial z-axis cannot be actuated and is always a constant during the motion of the ballbot. We consider the scenario where the relative orientation between the ball and the top is actuated as in Nagarajan et al. (2013) and Leutenegger and Fankhauser (2010). In other words, the control input belongs to the subbundle of the cotangent bundle of Q, characterised by the annihilator of the relative angular velocity ω_{tb}: $\tau' \in \{\sigma \in \mathfrak{so}^*(3) : \langle \sigma, \omega_{tb} \rangle = 0\}$, after its identification with $\mathbb{R}^3$. We notice that $\hat{\omega}_{tb} = Ad_{R_{st}^T} \left(\hat{\omega}_{sb} - \hat{\omega}_{st} \right)$ and using the dual of this mapping, we find the forced Euler–Lagrange equations of motion of the ballbot. We add the variations computed above and insert the rolling constraint (1) expressed as $\dot{p}_{sb} = r \left(\omega_{st} + \bar{\omega}_{tb} \right) \times e_3$ to arrive at,

$$\Big(I_t + m_t l^2 \left(I_3 - \Gamma \otimes \Gamma^\top \right) + I_b - (m_b + m_t) r^2 \hat{e}_3^2 - m_t r l \left(\hat{\Gamma} \hat{e}_3 + \hat{e}_3 \hat{\Gamma} \right) \Big) \dot{\omega}_{st} + \left(I_b - (m_b + m_t) r^2 \hat{e}_3^2 - m_t r l \hat{\Gamma} \hat{e}_3 \right) \dot{\bar{\omega}}_{tb}$$

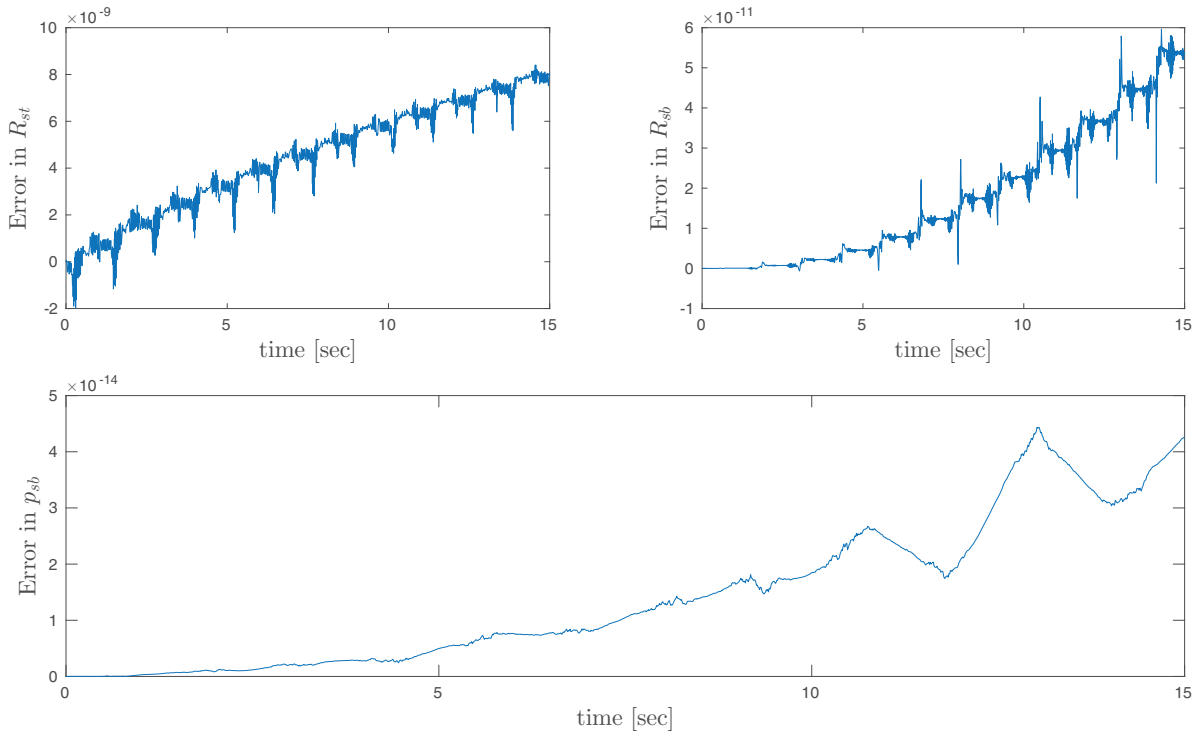

Figure 2. Error between Euler–Poincaré equations and the conventional Lagrangian approach.

$$+ m_t l^2 \langle \omega_{st}, \Gamma \rangle \hat{\Gamma}\omega_{st} + m_t r l \hat{e}_3 \hat{\omega}_{st}^2 \Gamma + \omega_{st} \times I_t \omega_{st} - \omega_{st} \times I_b \bar{\omega}_{tb} - m_t g l e_3 \times \Gamma = 0, \tag{9a}$$

$$\left(I_b - (m_b + m_t) r^2 \hat{e}_3^2 - m_t r l \hat{e}_3 \hat{\Gamma}\right) \dot{\omega}_{st} + \left(I_b - (m_b + m_t) r^2 \hat{e}_3^2\right) \dot{\bar{\omega}}_{tb} + m_t r l \hat{e}_3 \hat{\omega}_{st}^2 \Gamma - \bar{\omega}_{tb} \times I_b \omega_{st} = R_{st} \tau. \tag{9b}$$

Notice that this system is defined on $\mathfrak{so}(3) \times \mathfrak{so}(3) \times \mathbb{S}^2 \times \mathbb{R}^2$, which has dimension 10, as opposed to the original system, which is defined on TQ, with a dimension count of 16. In case the translational dynamics of the ball, which does not affect the stability of the system, is not considered, the reduced equations evolve on an eight-dimensional manifold, whereas the original equations of motion evolve on a 12-dimensional one.

We note the following definitions to be utilised as in the subsequent sections:

$$\begin{aligned} m_{11} &= I_t + m_t l^2 \left(I_3 - \Gamma \otimes \Gamma^\top\right) + I_b \\ &\quad - (m_b + m_t) r^2 \hat{e}_3^2 - m_t r l \left(\hat{\Gamma} \hat{e}_3 + \hat{e}_3 \hat{\Gamma}\right), \\ m_{12} &= I_b - (m_b + m_t) r^2 \hat{e}_3^2 - m_t r l \hat{\Gamma} \hat{e}_3, \\ m_{22} &= I_b - (m_b + m_t) r^2 \hat{e}_3^2. \end{aligned}$$

A comparison of the Euler–Poincaré dynamics and the conventional Euler–Lagrange equations derived using coordinates is made in Figure 2, where the errors in R_{st}, R_{sb}, and p_{sb} between the two approaches have been plotted when the ballbot is operated freely under its drift vector field. Since the numerical integration error margin to be tolerated has been selected to be 10^{-7}, these errors are well within the tolerance range.

2.4 2D dynamics

We are interested in finding out how the equations of motion restrict to the plane spanned by the inertial x–z axes. In particular, we are going to use coordinates (x, θ) on the circle for the rotation of the top with respect to the inertial frame and the rotation of the top with respect to the ball, respectively. With this choice, the relevant quantities take on the values

$$R_{st} = R_{e_2,x}, \ \omega_{st} = \dot{x} e_2; \quad R_{tb} = R_{e_2,\theta}, \ \omega_{sb} = \dot{\theta} e_2,$$

where $R_{e_2,\zeta}$ is the simple rotation matrix by ζ radians around the second standard basis vector e_2. When restricted to the plane, the nonholonomic constraint becomes a holonomic one, and is given by

$$\dot{p}_{sb} = r \omega_{sb} \times e_3 = \left[r \left(\dot{x} + \dot{\theta}\right) \ 0 \ 0 \right]^\top. \tag{10}$$

Using these quantities, the Lagrangian (5) restricted to the inertial x–z plane is computed to be

$$\begin{aligned} L = &\frac{1}{2}\left(I_t + m_t l^2 + m_t rl\cos(x) + I_b + (m_b + m_t)r^2\right)\dot{x}^2 \\ &+ \left(I_b + (m_b + m_t)r^2 + m_t rl\cos(x)\right)\dot{x}\dot{\theta} \\ &+ \frac{1}{2}\left(I_b + (m_b + m_t)r^2\right)\dot{\theta}^2 - m_t gl\cos x. \end{aligned}$$

We can either use the conventional Euler–Lagrange equations with coordinates $(x,\ \theta)$ or directly the coordinate-invariant equations (9) derived in the previous section to compute the equations of motion of the ballbot restricted to the plane. It is readily checked that these two distinct methods yield exactly the same equations, which are given by

$$\begin{aligned} &M(q)\ddot{q} + C(q,\dot{q})\dot{q} + g(q) \\ &:= \begin{bmatrix} \alpha + \gamma + 2\beta\cos x & \alpha + \beta\cos x \\ alpha + \beta\cos x & \alpha \end{bmatrix}\begin{bmatrix} \ddot{x} \\ ddot\theta \end{bmatrix} \\ &+ \begin{bmatrix} -\beta\sin x\dot{x} & 0 \\ -\beta\sin x\dot{x} & 0 \end{bmatrix}\begin{bmatrix} \dot{x} \\ dot\theta \end{bmatrix} \\ &+ \begin{bmatrix} -\mu\sin x \\ 0 \end{bmatrix} = \begin{bmatrix} 0 \\ 1 \end{bmatrix}\tau \end{aligned} \tag{11}$$

complemented by the rolling constraint (10). The various constants in these equations are given by $\alpha := I_{b,\,22} + (m_b + m_t)r^2$, $\beta := m_t rl$, $\gamma := I_{t,\,22} + m_t l^2$ and $\mu := m_t gl$. These equations correspond exactly to the ones given in Nagarajan et al. (2013).

3. Passivity based control design

When $\tau = 0$, we can determine the equilibria of the ballbot using the equations of motion (9) with the rolling contraint (1) and (7). Along with the fact that the inertial z-axis rotation of the ball is assumed to be stationary, the rolling constraints yields $\dot{p}_{sb} = 0 \Longleftrightarrow \omega_{sb} = \omega_{st} + \bar{\omega}_{tb} = 0$. Inserting $p_{sb} = $ constant and $\bar{\omega}_{tb} = 0$ into the equations of motion (9) along with $\omega_{st} \equiv 0$ yields $e_3 \times \Gamma = 0$. In other words, the uncontrolled equilibria of the ballbot are given by

$$\begin{aligned} E_{\pm} = \{&\left(p_{sb},\ \Gamma,\ \dot{p}_{sb},\ \omega_{sb},\ \omega_{st}\right) \in TQ : p_{sb} \\ &= \text{const},\ \ \Gamma = \pm e_3 \\ omega_{st} &= \bar{\omega}_{tb} = 0,\ \dot{p}_{sb} = 0\}. \end{aligned}$$

Notice that E_+ corresponds to the upward equilibrium point, that is, the top points in the inertial positive z-direction and E_- corresponds to the downward equilibrium point. The control objective is to asymptotically stabilise the set E_+.

3.1 Passivity and energy considerations for the 2D ballbot

Partial feedback linearisation of (11) is achieved by the following feedback:

$$\begin{aligned} \tau = &\left(\alpha - \frac{(\alpha + \beta\cos(x))^2}{\alpha + \gamma + 2\beta\cos(x)}\right)u \\ &+ \left(\frac{\alpha + \beta\cos(x)}{\alpha + \gamma + 2\beta\cos(x)} - 1\right)\beta\sin(x)\dot{x}^2 \\ &+ \frac{\mu\,(\alpha + \beta\cos(x))}{\alpha + \gamma + 2\beta\cos(x)}\sin(x). \end{aligned}$$

which yields the system,

$$\begin{aligned} &(\alpha + \gamma + 2\beta\cos(x))\,\ddot{x} - \beta\sin(x)\dot{x}^2 - \mu\sin(x) \\ &\quad = -(\alpha + \beta\cos(x))\,u, \end{aligned} \tag{12a}$$

$$\ddot{\theta} = u. \tag{12b}$$

The following are two passive outputs:

$$y_1 = \dot{\theta}, \tag{13a}$$

$$y_2 = -(\alpha + \beta\cos(x))\,\dot{x}. \tag{13b}$$

with the corresponding storage functions,

$$H_1 = \frac{1}{2}\dot{\theta}^2, \tag{14a}$$

$$H_2 = \frac{1}{2}(\alpha + \gamma + 2\beta\cos(x))\,\dot{x}^2 + \mu\cos(x). \tag{14b}$$

3.2 2D Energy-shaping control

Let us consider the following Lyapunov function candidate

$$\begin{aligned} H_d = &k_e\left(k_1 H_1 + k_2 H_2\right) + \frac{1}{2}k_k\left(k_1 y_1 + k_2 y_2\right)^2 \\ &+ \frac{1}{2}k_I\left(k_1\theta - k_2\left(\alpha x + \beta\sin(x)\right)\right)^2, \end{aligned} \tag{15}$$

Notice that this Lyapunov function candidate comes from a desired energy function that can be written as $H_d = \frac{1}{2}[\,\dot{\theta}\ \dot{x}\,]M_d\begin{bmatrix} \dot{\theta} \\ dotx \end{bmatrix} + V_d$, where

$$\begin{aligned} M_{d,11} &= k_e k_1 + k_1^2 k_k, \\ M_{d,12} &= -k_1 k_2 k_k\left(\alpha + \beta\cos(x)\right), \\ M_{d,22} &= k_e k_2\left(\alpha + \gamma + 2\beta\cos(x)\right) + k_2^2 k_k\left(\alpha + \beta\cos(x)\right)^2, \\ V_d &= k_e k_2\mu\cos(x) + \frac{1}{2}k_I\left(k_1\theta - k_2\left(\alpha x + \beta\sin(x)\right)\right)^2. \end{aligned}$$

The conditions under which M_d and V_d can be selected such that H_d is a Lyapunov function are developed in the next subsection for the 3D-dynamics of the ballbot. Taking the Lie derivative of (15) along the solutions of (12), we get

$$\begin{aligned}\dot{H}_d = \left(k_1 y_1 + k_2 y_2\right)\Bigg[&\left(k_e + k_1 k_k + k_2 k_k \frac{(\alpha + \beta\cos(x))^2}{\alpha + \gamma + 2\beta\cos(x)}\right) u \\ &+ k_2 k_k \Bigg(- (\alpha + \beta c_x)\left(\frac{\beta s_x}{\alpha + \gamma + 2\beta c_x}\dot{x}^2 \right. \\ &\left. + \frac{\mu s_x}{\alpha + \gamma + 2\beta c_x}\right) + \beta s_x \dot{x}^2\Bigg) \\ &+ k_I\left(k_1\theta - k_2\left(\alpha x + \beta s_x\right)\right)\Bigg].\end{aligned}$$

Once we select the control as follows:

$$\begin{aligned}u = -\frac{1}{k}\Bigg[&k_2 k_k \Bigg(- (\alpha + \beta c_x)\left(\frac{\beta s_x}{\alpha + \gamma + 2\beta c_x}\dot{x}^2 \right. \\ &\left. + \frac{\mu s_x}{\alpha + \gamma + 2\beta c_x}\right) + \beta s_x \dot{x}^2\Bigg) \\ &+ k_I\left(k_1\theta - k_2\left(\alpha x + \beta s_x\right)\right) + k_p\left(k_1 y_1 + k_2 y_2\right)\Bigg]\end{aligned}$$

where $k = k_e + k_1 k_k + k_2 k_k \frac{(\alpha+\beta c_x)^2}{\alpha+\gamma+2\beta c_x}$, the time derivative of H_d becomes

$$\dot{H}_d = -k_p\left(k_1 y_1 + k_2 y_2\right)^2 \leq 0.$$

Once the detectability of the output $y = k_1 y_1 + k_2 y_2$ is proven, this implies that the desired equilibrium point is asymptotically stable. The detectability of this output is proven in the next section for the full dynamics of the ballbot. It is omitted in this section because that calculation can be applied to the 2D dynamics verbatim.

3.3 Passivity and energy considerations for the 3D ballbot

Partial feedback linearisation of the equations of motion (9) on the second factor yields,

$$\begin{aligned}&\left(I_t + m_t l^2\left(I_3 - \Gamma\otimes\Gamma^\top\right) + I_b\right. \\ &\quad\left. -(m_b + m_t) r^2 \hat{e}_3^2 - m_t r l\left(\hat{\Gamma}\hat{e}_3 + \hat{e}_3\hat{\Gamma}\right)\right)\dot{\omega}_{st} \\ &\quad + m_t l^2\left\langle\omega_{st}, \Gamma\right\rangle\hat{\Gamma}\omega_{st} + m_t r l \hat{e}_3\hat{\omega}_{st}^2\Gamma + \omega_{st} \\ &\quad \times I_t\omega_{st} - \omega_{st}\times I_b\bar{\omega}_{tb} - m_t g l e_3\times\Gamma \\ &= -\left(I_b - (m_b + m_t) r^2\hat{e}_3^2 - m_t r l\hat{\Gamma}\hat{e}_3\right)u, \qquad (16a)\end{aligned}$$

$$\dot{\bar{\omega}}_{tb} = u \qquad (16b)$$

where the feedback linearising torque is given by

$$\begin{aligned}\tau = R_{st}^\top&\left(m_{22} - m_{12}^\top m_{11}^{-1} m_{12}\right) \\ &\times\Bigg(u + m_t r l\left(I_3 - m_{12}^\top m_{11}^{-1}\right)\hat{e}_3\hat{\omega}_{st}^2\Gamma \\ &- m_{12}^\top m_{11}^{-1} m_t l^2\left\langle\omega_{st}, \Gamma\right\rangle\hat{\Gamma}\omega_{st} \\ &+ m_{12}^\top m_{11}^{-1} m_t g l\left(e_3\times\Gamma\right)\Bigg).\end{aligned}$$

The following are two passive outputs:,

$$y_1 = \bar{\omega}_{tb}, \qquad (17a)$$

$$y_2 = -\left(I_b - (m_b + m_t) r^2\hat{e}_3^2 - \beta\hat{e}_3\hat{\Gamma}\right)\omega_{st} \qquad (17b)$$

with the corresponding storage functions,

$$H_1 = \frac{1}{2}\bar{\omega}_{tb}\cdot\bar{\omega}_{tb}, \qquad (18a)$$

$$\begin{aligned}H_2 = \frac{1}{2}\omega_{st}\cdot&\left(I_b - (m_b + m_t) r^2\hat{e}_3^2 - \beta\left(\hat{\Gamma}\hat{e}_3 + \hat{e}_3\hat{\Gamma}\right)\right. \\ &\left. + I_t + m_t l^2 I_3\right)\omega_{st} - \frac{1}{2} m_t l^2\left(\omega_{st}\cdot\Gamma\right)^2 + \mu e_3\cdot\Gamma.\end{aligned} \qquad (18b)$$

The passivity of the pair (y_1, H_1) is readily seen.

$$\frac{\mathrm{d}H_1}{\mathrm{d}t} = \left\langle\bar{\omega}_{tb}, u\right\rangle = \left\langle y_1, u\right\rangle.$$

To prove the same statement for the pair (y_2, H_2), we calculate

$$\begin{aligned}\frac{\mathrm{d}H_2}{\mathrm{d}t} &= \omega_{st}\cdot\Big[\left(I_b - (m_b + m_t) r^2\hat{e}_3^2 - \beta\left(\hat{\Gamma}\hat{e}_3 + \hat{e}_3\hat{\Gamma}\right)\right. \\ &\quad\left. + I_t + m_t l^2\right)\dot{\omega}_{st} - \mu e_3\times\Gamma \\ &\quad + \frac{1}{2}\beta\left(\Gamma\times\left(\omega_{st}\times\left(e_3\times\omega_{st}\right)\right)\right. \\ &\quad\left. - e_3\times\left(\omega_{st}\times\left(\Gamma\times\omega_{st}\right)\right)\right)\Big] \\ &= \omega_{st}\cdot\Bigg[- \left(I_b - (m_b + m_t) r^2\hat{e}_3^2\right. \\ &\quad\left. - \beta\hat{\Gamma}\hat{e}_3\right)u - \beta\left(e_3\times\left(\omega_{st}\times\left(\omega_{st}\times\Gamma\right)\right)\right) \\ &\quad - \frac{1}{2}\beta\left(2e_3\times\left(\omega_{st}\times\left(\Gamma\times\omega_{st}\right)\right)\right)\Bigg] \\ &= \left\langle -\left(I_b - (m_b + m_t) r^2\hat{e}_3^2 - \beta\hat{e}_3\hat{\Gamma}\right)\omega_{st}, u\right\rangle = \left\langle y_2, u\right\rangle,\end{aligned}$$

where the second to the last step follows by noticing that the first two terms in the final expression below are orthogonal to ω_{st}.

$$\begin{aligned}&\Gamma \times (\omega_{st} \times (e_3 \times \omega_{st}))\\ &= -\omega_{st} \times ((e_3 \times \omega_{st}) \times \Gamma) - (e_3 \times \omega_{st}) \times (\Gamma \times \omega_{st})\\ &= -\omega_{st} \times ((e_3 \times \omega_{st}) \times \Gamma)\\ &\quad -\omega_{st} \times ((\Gamma \times \omega_{st}) \times e_3) - e_3 \times (\omega_{st} \times (\Gamma \times \omega_{st}))\,.\end{aligned}$$

Lemma 3.1: *The integrals of the passive outputs can be computed to be,*

$$\dot{\bar{\theta}}_{tb} = y_1, \tag{19a}$$

$$\frac{\mathrm{d}}{\mathrm{d}t}\left\{-m_{22}\theta_{st} - \beta e_3 \times \Gamma\right\} = y_2. \tag{19b}$$

Proof: We first compute the integral of part of the second output, $-\beta e_3 \times (\Gamma \times \omega_{st})$. Let $\Phi(\Gamma, \omega_{st}) = \beta e_3 \times \Gamma$, then

$$\frac{\mathrm{d}\Phi}{\mathrm{d}t} = \beta\left(e_3 \times \dot{\Gamma}\right) = -\beta\left(e_3 \times (\Gamma \times \omega_{st})\right). \tag{20}$$

To locally express the integral of the remaining terms, we use the exponential mapping from $\mathfrak{so}(3)$ to $SO(3)$ to express the rotation so that

$$R_{st} = \mathrm{e}^{\hat{\theta}_{st}}, \quad R_{tb} = \mathrm{e}^{\hat{\theta}_{tb}} = \mathrm{e}^{-\hat{\theta}_{st}}\mathrm{e}^{\hat{\theta}_{sb}}.$$

Upon differentiation and utilisation of the rigid body kinematics (2), we have

$$\begin{aligned}&\hat{\omega}_{st} = \dot{R}_{st}R_{st}^{\top} = \dot{\hat{\theta}}_{st},\\ &hat\bar{\omega}_{tb} = Ad_{R_{st}}\hat{\omega}_{tb} = Ad_{R_{st}}\left(\dot{R}_{tb}R_{tb}^{\top}\right) = -\dot{\hat{\theta}}_{st} + \dot{\hat{\theta}}_{sb} =: \dot{\hat{\bar{\theta}}}_{tb}.\end{aligned}$$

Combining these with (20) yields the assertions of the lemma. ■

3.4 3D Energy-shaping control

Let us consider the following Lyapunov function candidate:

$$\begin{aligned}H_d = k_e\left(k_1H_1 + k_2H_2\right) + \frac{1}{2}\|k_1y_1 + k_2y_2\|^2_{K_k}\\ + \frac{1}{2}\|k_1\bar{\theta}_{tb} + k_2\left(-m_{22}\theta_{st} - \beta e_3 \times \Gamma\right)\|^2_{K_I}.\end{aligned} \tag{21}$$

Notice that this Lyapunov function candidate comes from a desired energy function that can be written as $H_d = \frac{1}{2}\left[\begin{smallmatrix}\omega_{tb} & \omega_{st}\end{smallmatrix}\right]M_d\left[\begin{smallmatrix}\omega_{tb}\\ omega_{st}\end{smallmatrix}\right] + V_d$, where,

$$M_d = \begin{bmatrix}k_ek_1I_3 + k_1^2K_k & -k_1k_2K_km_{12}^{\top}\\ -k_1k_2m_{12}K_k & k_ek_2m_{11} + k_2^2m_{12}K_km_{12}^{\top}\end{bmatrix}, \tag{22a}$$

$$V_d = k_ek_2V + \frac{1}{2}\|k_1\bar{\theta}_{tb} + k_2\left(-m_{22}\theta_{st} - \beta e_3 \times \Gamma\right)\|^2_{K_I}. \tag{22b}$$

Let $q^* = (R_{st}, R_{tb}, \omega_{st}, \bar{\omega}_{tb}) = \left(\mathrm{e}^{\rho\hat{e}_3}, \mathrm{e}^{\sigma\hat{e}_3}, 0, 0\right)$, for some $\rho, \sigma \in \mathbb{R}$ are constants. In order for H_d to qualify as a Lyapunov function, we need to make sure that $M_d(q^*) \succ 0$, $\delta V_d(q^*) = 0$, $\delta^2V_d(q^*)$ is full rank along the directions orthogonal to the combined, but functionally related rotation of the ball and the top along the inertial vertical axis, and $\dot{H}_d \leq 0$. As long as the yaw rotation of the ball is restricted by its friction with the ground, by Lagrange–Dirichlet stability criterion, these conditions will ensure that both the ball and the top will converge to the desired orientation.

Theorem 3.1: *At q^*, V_d has a global minimum V_d^*, which is shared by a line of points characterised by a combined rotation of the ball and the top along the inertial vertical axis.*

Proof: We observe from the expression of V_d that it achieves a minimum only if each term individually achieves a minimum. While the minimum of the second term is zero, the minimum $k_ek_2\mu$ of the first term $k_ek_2\mu e_3 \cdot \Gamma$ is attained when $\Gamma = e_3$, provided that $k_2 < 0$ and $k_e > 0$. Computing the first variation of V_d yields

$$\begin{aligned}\delta V_d = k_ek_2\mu\eta_{st} \cdot (\Gamma \times e_3) + (k_1\bar{\theta}_{tb} - k_2(m_{22}\theta_{st}\\ +\beta e_3 \times \Gamma))^{\top}K_I(k_1\bar{\eta}_{tb} - k_2(m_{22} - \beta\hat{e}_3\hat{\Gamma})\eta_{st}).\end{aligned}$$

which vanishes at q^*. Note that when $\theta_{st} = 0$, it follows that $\Gamma = R_{st}e_3 = \mathrm{e}^{\hat{\theta}_{st}}e_3 = \mathrm{e}^{\hat{0}}e_3 = e_3$.

Computing the second variation δ^2V_d of V_d at $q^* = 0$ yields

$$\delta^2V_d = k_ek_2\eta_{st} \cdot \hat{e}_3^2\eta_{st} + \|k_1\bar{\eta}_{tb} - k_2\left(m_{22} - \beta\hat{e}_3^2\right)\eta_{st}\|^2_{K_I}.$$

This expression shows that δ^2V_d is positive semidefinite and is degenerate only on the subspace spanned by $\eta_{st} = e_3$ and $\bar{\eta}_{tb} = \frac{k_2}{k_1}m_{22}e_3$. Since m_{22} is a diagonal matrix, $\bar{\eta}_{tb}$ is a multiple of e_3 by a negative constant. ■

The assumption that the yaw rotation of the ball is constrained by frictional forces implies that $\eta_{sb} \cdot e_3 = 0$. Since $\bar{\eta}_{tb} = -\eta_{st} + \eta_{sb}$, it follows that $\bar{\eta}_{tb} \cdot e_3 = -\eta_{st} \cdot e_3$. Notice that this subspace and the nullspace of δ^2V_d intersect only at the zero section of the tangent bundle (state space).

Theorem 3.2: *If the ballbot is strongly inertially coupled (Spong, 1994), i.e. rank$(m_{12}(q)) = 3$, then appropriate gains k_e, k_1, k_2, K_k can be chosen such that $M_d(q) \succ 0$.*

Proof: M_d is positive definite if $k_e k_1 I_3 + k_1^2 K_k \succ 0$ and $\Delta_{11} \succ 0$, where Δ_{11} is the Schur-complement of the (1, 1) block of M_d, that is,

$$\Delta_{11} = k_2 \left(k_e m_{11} + k_2 m_{12} K_k m_{12}^\top\right) - k_1 k_2^2 m_{12} K_k \left(k_e I_3 + k_1 K_k\right)^{-1} K_k m_{12}^\top.$$

The condition that $k_e k_1 I_3 + k_1^2 K_k \succ 0$ holds if k_e, $k_1 > 0$ and $K_k \succ 0$. These constraints on the gains will be in force in the sequel. Let $\underline{\lambda}_k$ be the smallest eigenvalue of K_k, $\bar{\lambda}_{11}$ denote the maximum of eigenvalue of m_{11}, and $\underline{\lambda}_{12}$ denote the minimum eigenvalue of $m_{12} m_{12}^\top$ as Γ varies over $\mathbb{S}^2$. Note that when the hypothesis of the theorem holds, then $\underline{\lambda}_{12}$ is bounded away from zero. Since $k_2 < 0$ and $m_{11} \succ 0$, we have the following implications:

$$\begin{aligned}
\Delta_{11} \succ 0 \Leftrightarrow\ & k_e m_{11} \\
& + k_2 m_{12} K_k \left(I_3 - k_1 \left(k_e I_3 + k_1 K_k\right)^{-1} K_k\right) m_{12}^\top \prec 0 \\
\Leftarrow\ & k_e \bar{\lambda}_{11} I_3 + k_2 \underline{\lambda}_k \left(1 - \frac{k_1 \underline{\lambda}_k}{k_e + k_1 \underline{\lambda}_k}\right) m_{12} m_{12}^\top \prec 0 \\
\Leftarrow\ & k_e \bar{\lambda}_{11} + k_2 \underline{\lambda}_k \left(1 - \frac{k_1 \underline{\lambda}_k}{k_e + k_1 \underline{\lambda}_k}\right) \underline{\lambda}_{12} < 0.
\end{aligned}$$

The last implication shows that choosing the quantity $\frac{|k_2| \underline{\lambda}_k}{k_e}$ large enough ensures that the desired mass matrix M_d is positive definite at all points q where the system is strongly inertially coupled. ■

Whether or not the system is strongly inertially coupled depends on the design of the mechanism. If the mass and inertia of the ball is large enough with respect to the mass of the top, then this property holds everywhere in the configuration space and therefore the following control law achieves global asymptotic stability for those mechanism designs.

Proposition 3.1: *Consider the partially feedback linearised dynamics of the ballbot* (16) *in closed loop with the control law*

$$u = -K^{-1} \left[S + K_p \left(k_1 y_1 + k_2 y_2\right)\right], \tag{23}$$

with the expressions for K and S are as given in the proof, $K_p \succ 0$, and k_1, k_2 satisfy the conditions that render $M_d \succ 0$, $\delta V_d(q^*) = 0$, and $\delta^2 V_d(q^*) \succ 0$.

Then, q^* is an asymptotically stable equilibrium of the closed-loop system.

Proof: Taking the Lie derivative of (21) along the solutions of (16), we get

$$\begin{aligned}
\dot{H}_d = & \left\langle k_1 y_1 + k_2 y_2, \left[\left(k_e I_3 + k_1 K_k + k_2 K_k m_{12}^\top m_{11}^{-1} m_{12}\right) u \right.\right. \\
& + k_2 K_k \left(-\dot{m}_{12}^\top \omega_{st} + m_{12}^\top m_{11}^{-1} \left(c_1 + g_1\right)\right) \\
& \left.\left. + K_I \left(k_1 \bar{\theta}_{tb} + k_2 \left(-m_{22} \theta_{st} - \beta e_3 \times \Gamma\right)\right)\right]\right\rangle \\
= & \left\langle k_1 y_1 + k_2 y_2, K u + S \right\rangle,
\end{aligned}$$

where $c_1 = m_t l^2 \left\langle \omega_{st}, \Gamma \right\rangle \hat{\Gamma} \omega_{st} + \beta \hat{e}_3 \hat{\omega}_{st}^2 \Gamma + \omega_{st} \times I_t \omega_{st} - \omega_{st} \times I_b \hat{\omega}_{tb}$, $g_1 = -\mu e_3 \times \Gamma$. We thus select

$$u = -K^{-1} \left[S + K_p \left(k_1 y_1 + k_2 y_2\right)\right], \tag{24}$$

where $K = \left(k_e I_3 + k_1 K_k + k_2 K_k m_{12}^\top m_{11}^{-1} m_{12}\right)$, S consists of all the terms not multiplied by u in the second factor of the natural pairing and $K_p \succ 0$, yielding

$$\dot{H}_d = -\left\| k_1 y_1 + k_2 y_2 \right\|_{K_p}^2.$$

This implies that $k_1 y_1 + k_2 y_2 \underset{[t \to \infty]}{\longrightarrow} 0$. Let us analyse the smallest invariant set within $\mathcal{E} = \{k_1 y_1 + k_2 y_2 = 0\}$. We have

$$0 = k_1 K_k \dot{y}_1 + k_2 K_k \dot{y}_2 = \left(k_1 K_k + k_2 K_k m_{12}^\top m_{11}^{-1} m_{12}\right) u + \Delta_1,$$

where $\Delta_1 = k_2 K_k \left(-\dot{m}_{12}^\top \omega_{st} + m_{12}^\top m_{11}^{-1} \left(c_1 + g_1\right)\right)$. Thus, we can write the above equation as $(K - k_e I) u = -\Delta_1$. From the control law (23), we have $Ku = -(\Delta_1 + \Delta_2)$, where $\Delta_2 = K_I \left(k_1 \bar{\theta}_{tb} + k_2 \left(-m_{22} \theta_{st} - \beta e_3 \times \Gamma\right)\right)$. Therefore, from the following two equations,

$$\begin{aligned}
\left(K - k_e I\right) u &= -\Delta_1 \\
K u &= -\left(\Delta_1 + \Delta_2\right),
\end{aligned}$$

we deduce that $u = -\frac{\Delta_2}{k_e}$ on $\mathcal{E}$. Plugging this in (16) shows that the first of these equations is unstable unless $u = \Delta_2 = 0$. This implies $\bar{\omega}_{tb} = \text{constant} = 0$, which, in turn, implies $\omega_{st} = 0$ because otherwise its dynamics would again be unstable. This discussion shows that the system asymptotically converges to an equilibrium point. Since the closed-loop system comes from a Lagrangian system, it is readily shown that, the only stable equilibrium point is the upward equilibrium point, with $\theta_{st} = (0, 0, \text{constant})$ and $\bar{\theta}_{tb} = (0, 0, \text{constant})$, where the inertial z-axis rotation of the system goes to a certain constant because this motion is uncontrollable. ■

3.5 Controlling the ball position

We can use a similar technique as in Section 3.4 to control the position of the ball as well as the upward equilibrium point of the top. In order to do this, we start from Equations (16) and switch to the error system dynamics, with the error defined by $\bar{e}_{tb} := \bar{\omega}_{tb} - \bar{\omega}_{tb}^d$, where $\bar{\omega}_{tb}^d$ is the desired angular velocity of the ball with respect to the top expressed in the spatial frame. We compute this quantity from the desired angular velocity of the ball with respect to the spatial frame, ω_{sb}^d, which is, in turn, computed from the rolling constraint (1). In order for $p_{sb} \to p_{sb}^d$, where p_{sb}^d is the desired position of the ball on the x–y plane (the

z component is a constant), we would like the rolling constraint equation (1) to look like

$$\dot{p}_{sb} = r\omega_{sb}^d \times e_3 = k_t \hat{e}_3^2 \left(p_{sb} - p_{sb}^d\right).$$

As a result, we set $\omega_{sb}^d = -\frac{k_t}{r}\hat{e}_3\left(p_{sb} - p_{sb}^d\right)$, where k_t is a positive constant. This implies that the desired angular velocity of the ball with respect to the top expressed in the spatial frame is $\bar{\omega}_{tb}^d = \omega_{sb}^d - \omega_{st}$. We use (1) in the time derivative of this relation to get

$$\dot{\bar{\omega}}_{tb}^d = \dot{\omega}_{sb}^d - \dot{\omega}_{st} = k_t \hat{e}_3^2 \left(\bar{\omega}_{tb} + \omega_{st}\right) - \dot{\omega}_{st}. \tag{25}$$

We set the control u in Equation (16) to $u = \dot{\bar{\omega}}_{tb}^d + \upsilon$ which yields the error system dynamics,

$$\left(m_{11} - m_{12}\right)\dot{\omega}_{st} + c_2 + g_1 = -m_{12}\upsilon, \tag{26a}$$

$$\dot{\bar{e}}_{tb} = \upsilon. \tag{26b}$$

where $c_2 = c_1 + k_t m_{12}\hat{e}_3^2\left(\bar{\omega}_{tb} + \omega_{st}\right)$. Solving (26) for $\dot{\omega}_{st}$ and substituting into (25), we derive the form of the control u as

$$\begin{aligned} u = &\left(I_3 + \left(m_{11} - m_{12}\right)^{-1} m_{12}\right)\upsilon \\ &+ \left(m_{11} - m_{12}\right)^{-1}\left(c_2 + g_1\right) + k_t \hat{e}_3^2\left(\bar{\omega}_{tb} + \omega_{st}\right). \end{aligned}$$

We identify a passive output $y_1 = \bar{e}_{tb}$ with the storage function $H_1 = \frac{1}{2}\bar{e}_{tb} \cdot \bar{e}_{tb}$. We keep the second output $y_2 = -m_{12}^\top \omega_{st}$ and modify its storage to $H_2' = H_2 - \omega_{st} \cdot m_{12}\omega_{st}$. Note that this output with the storage function H_2' is not passive anymore due to the additional terms appearing in c_2. It is also important to note that, we do not need to asymptotically stabilise the orientation of the ball to a desired value. We would rather asymptotically stabilise $\bar{e}_{tb}$ to zero, which implies $\omega_{sb} \to \omega_{sb}^d$, which, in turn, asymptotically stabilises p_{sb} to p_{sb}^d. This observation implies that, we only need to devise a desired potential energy which has $\Gamma = e_3$, a point of minimum. This is easily achieved by setting $V_d = k_e k_2 V$. Recall that the product $k_e k_2$ is negative and since the original potential energy V has a minimum at $\Gamma = -e_3$, this desired potential energy is good enough.

To shape the kinetic energy of the system, we use the same desired mass matrix as the one (22) used in the previous subsection. We use the following desired Hamiltonian (energy) for the closed-loop system

$$\begin{aligned} H_d = &\, k_e\left(k_1 H_1 + k_2 H_2'\right) + \frac{1}{2}\left\|k_1 y_1 + k_2 y_2\right\|_{K_k}^2 \\ &+ \frac{1}{2}\left\langle p_{sb} - p_{sb}^d, p_{sb} - p_{sb}^d\right\rangle. \end{aligned}$$

Proceeding analogously to Proposition 3.1, we compute the time derivative of H_d to be

$$\begin{aligned} \dot{H}_d = &\left\langle k_1 y_1 + k_2 y_2, \left[\left(k_e I_3 + k_1 K_k\right.\right.\right. \\ &+ k_2 K_k m_{12}^\top \left(m_{11} - m_{12}\right)^{-1} m_{12}\big)\upsilon \\ &+ k_2 K_k\left(-\dot{m}_{12}^\top \omega_{st} + m_{12}^\top \left(m_{11} - m_{12}\right)^{-1}\left(c_2 + g_1\right)\right)\left.\left.\right]\right\rangle \\ &- \frac{\beta}{2}\left\langle \omega_{st}, \hat{e}_3^2 \hat{\omega}_{st}^2 \Gamma\right\rangle \\ &+ \left\langle -k_e k_t \hat{e}_3^2\left(y_1 - \frac{k_t}{r}\hat{e}_3\left(p_{sb} - p_{sb}^d\right)\right), k_2 y_2\right\rangle \\ &+ \left\langle k_t \hat{e}_3^2\left(p_{sb} - p_{sb}^d\right), p_{sb} - p_{sb}^d\right\rangle + \left\langle r y_1, \hat{e}_3\left(p_{sb} - p_{sb}^d\right)\right\rangle, \end{aligned}$$

where the second and third natural pairings arise because of the extra terms in the new Coriolis term, c_2. We select the control υ as

$$\upsilon = -K_b^{-1}\left[S_b + K_p\left(k_1 y_1 + k_2 y_2\right) + \frac{k_e k_t^2}{r}\hat{e}_3^2\left(p_{sb} - p_{sb}^d\right)\right], \tag{27}$$

where $K_b = \left(k_e I_3 + k_1 K_k + k_2 K_k m_{12}^\top \left(m_{11} - m_{12}\right)^{-1} m_{12}\right)$, S_b consists of all the terms not multiplied by υ in the second factor of the first natural pairing and $K_p \succ 0$. This selection yields to the following expression for the time derivative of H_d along the solutions of the system

$$\begin{aligned} \dot{H}_d = &-\left\|k_1 y_1 + k_2 y_2\right\|_{K_p}^2 + k_e k_2 k_t\left\langle \hat{e}_3^2 y_1, y_2\right\rangle \\ &- \frac{\beta}{2}\left\langle \omega_{st}, \hat{e}_3^2 \hat{\omega}_{st}^2 \Gamma\right\rangle + k_t\left\langle \hat{e}_3^2\left(p_{sb} - p_{sb}^d\right), p_{sb} - p_{sb}^d\right\rangle \\ &+ \left\langle\left(r - \frac{k_1 k_e k_t^2}{r}\right), \hat{e}_3\left(p_{sb} - p_{sb}^d\right)\right\rangle. \end{aligned}$$

Selecting $k_t = \frac{r}{\sqrt{k_1 k_e}}$ ensures that the last natural pairing in this expression vanishes. While the first natural pairing may be absorbed into the very first term, using the Cauchy–Schwarz inequality, by a proper selection of the gain K_p, the second natural pairing satisfies the linear growth condition as long as strong inertial coupling condition is satisfied. As a result, this pairing may also be dominated by the first term semi-globally by increasing the magnitude of the gain k_2. These arguments prove that $\dot{H}_d \leq 0$. Since the detectability of the output $y = k_1 y_1 + k_2 y_2$ is proven in exactly the same way as in the proof of Proposition 3.1, we can summarise the result in the following proposition:

Proposition 3.2: *Consider the partially feedback linearised dynamics of the ballbot* (16) *in closed loop with the control law,*

$$\upsilon = -K_b^{-1}\left[S_b + K_p\left(k_1 y_1 + k_2 y_2\right) + \frac{k_e k_t^2}{r}\hat{e}_3^2\left(p_{sb} - p_{sb}^d\right)\right], \tag{28a}$$

Table 1. System parameters.

Parameter	*Symbol*	*Value*
Ball radius	r	*0.1058 (m)*
Ball mass	m_b	*244 (kg)*
Ball inertia	I_b	*1.821 (kg m^2)*
Top centre of mass height	l	*0.69 (m)*
Roll moment of inertia	$I_{t,11}$	*12.59 (kg m^2)*
Pitch moment of inertia	$I_{t,22}$	*12.48 (kg m^2)*
Yaw moment of inertia	$I_{t,33}$	*0.66 (kg m^2)*
Top mass	m_t	*51.66 (kg)*

$$u = \left(I_3 + (m_{11} - m_{12})^{-1} m_{12}\right) v + (m_{11} - m_{12})^{-1} \left(c_2 + g_1\right) + k_t \hat{e}_3^2 \left(\bar{\omega}_{tb} + \omega_{st}\right). \tag{28b}$$

with the expressions for K_b, S_b and k_t are as given above the proposition, $K_p \succ 0$, and k_1, k_2 satisfy the conditions that render $M_d \succ 0$, $\delta V_d(\Gamma = e_3) = 0$, and $\delta^2 V_d(\Gamma = e_3) \succ 0$.

Then, $\Gamma = e_3$, $\omega_{st} = 0$, $\bar{\omega}_{tb} = 0$, and $p_{sb} = p_{sb}^d$ is an asymptotically stable equilibrium of the closed-loop system.

Remark 3.1: Although the control design in the section is inspired by the development in Donaire et al. (2016), the technique presented in that work cannot be applied verbatim. The fundamental reason for this shortcoming is that the dynamics (9) is not derived directly from Euler–Lagrange equations, but are reduced to yield the Euler–Poincaré equations. Consequently, the construction of a second passive output in (17), a corresponding storage function in (18) and an integral of this passive output (19)

Table 2. Initial conditions and control gains.

	Initial conditions		*Control gains*		
Simulation 1	$x(0) = \frac{2\pi}{3}$	$\theta(0) = 4\pi$	$k_1 = 5$	$k_2 = -70$	$k_e = 20$
	$\dot{x}(0) = 0$	$\dot{\theta} = 0$	$k_k = 11$	$k_p = 10$	$k_l = 1$
Simulation 2	$R_{st}(0) = R_{y,\frac{\pi}{3}} R_{x,-\frac{\pi}{2}}$	$R_{sb}(0) = I_3$	$k_1 = 5$	$k_2 = -70$	$k_e = 20$
	$\omega_{st}(0) = \omega_{sb} = 0$	$p_{sb} = 0$	$K_k = 11I_3$	$K_p = 10I_3$	$K_l = I_3$
Simulation 3	$R_{st}(0) = R_{z,\frac{4\pi}{3}} R_{y,1.74} R_{x,1}$	$R_{sb}(0) = I_3$	$k_1 = 5$	$k_2 = -70$	$k_e = 20$
	$\omega_{st}(0) = \omega_{sb} = 0$	$\tilde{p}_{sb}(0) = (0.25, 0.4, 0)$	$K_k = 11I_3$	$K_p = 7.5I_3$	$k_t = \frac{r}{\sqrt{k_l k_e}}$

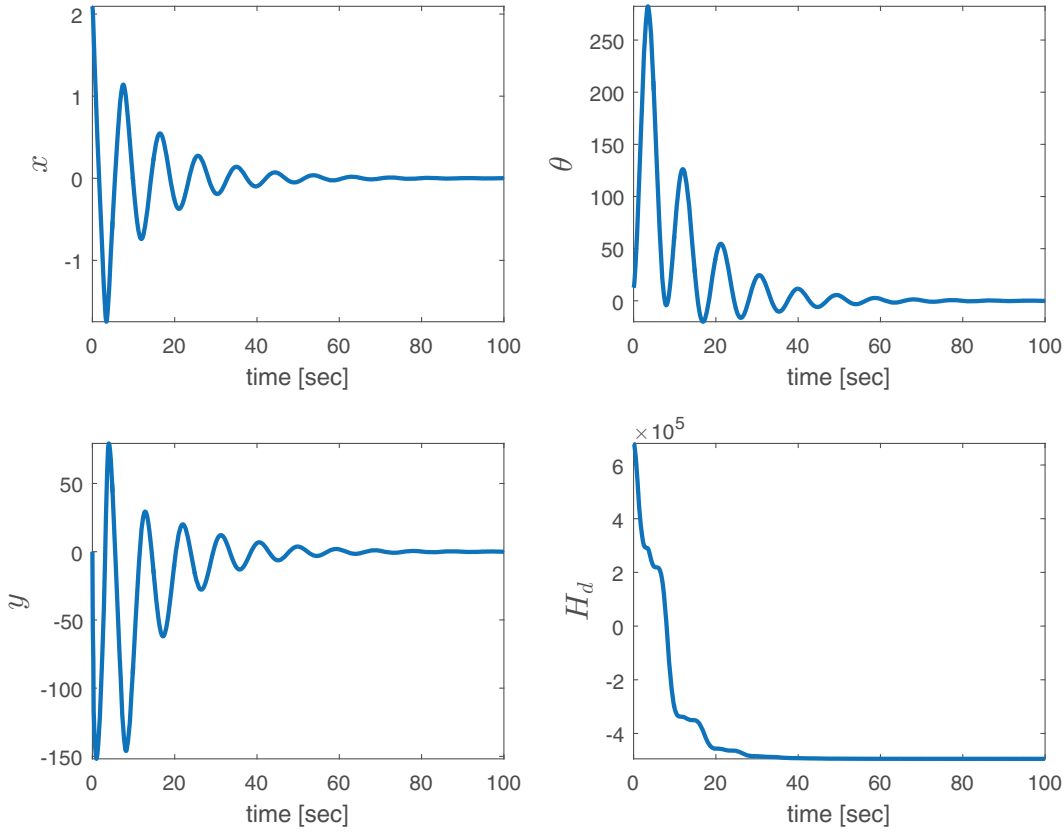

Figure 3. Asymptotic stabilisation of the 2D Ballbot.

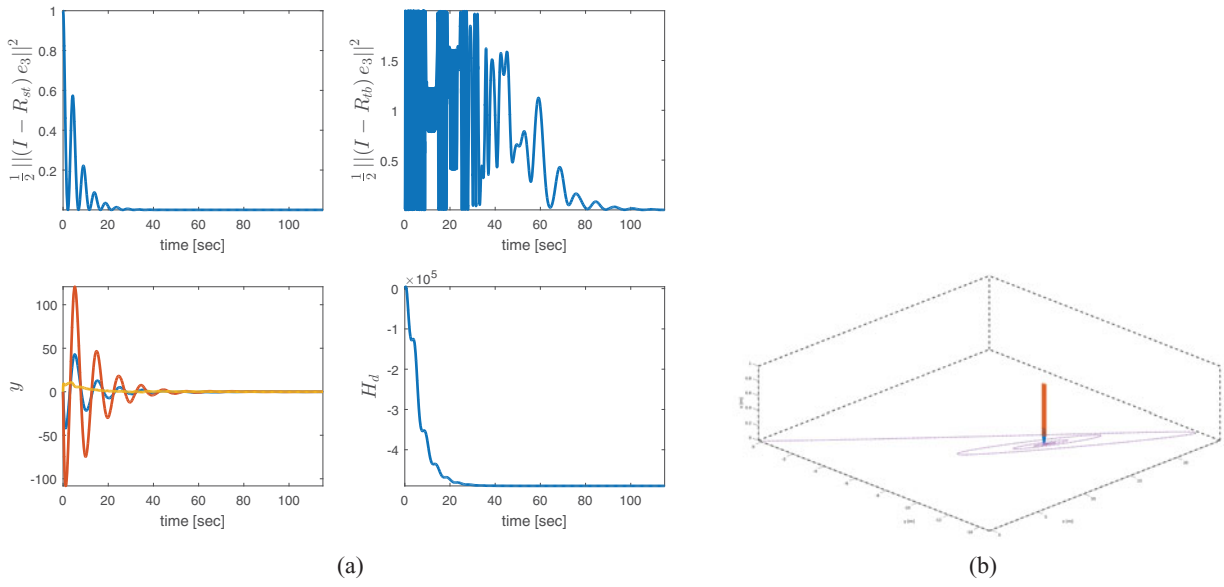

Figure 4. Asymptotic orientation stabilisation of the 3D ballbot. (a) Time evolution of quantities of interest, (b) the path tracked by the ballbot.

has to be novelly performed. Once these quantities have been obtained, we are able to construct the Lyapunov function (21).

4. Numerical examples

The inertial properties of the ballbot that are utilised in the simulations are given in Table 1.

First, simulation results for the ballbot whose dynamics is restricted to the two-dimensional x–z plane are presented. The initial conditions and the control gains used in the simulation are given in the first row of Table 2. The corresponding simulation results are shown in Figure 3. The top two plots illustrate the convergence of the orientation of the top and the ball; in other words, the fact that $(x, \theta) \to 0$. The bottom left plot shows the evolution of the passive output $y = k_1 y_1 + k_2 y_2$, while the bottom right plot shows the evolution of the closed-loop energy functional H_d (15).

Second, simulation results are presented that show the response of the ballbot to a feedback control (23). In this simulation, the initial conditions and the control gains are given by the second row of Table 2. Notice that the initial conditions are quite far away from the desired upward

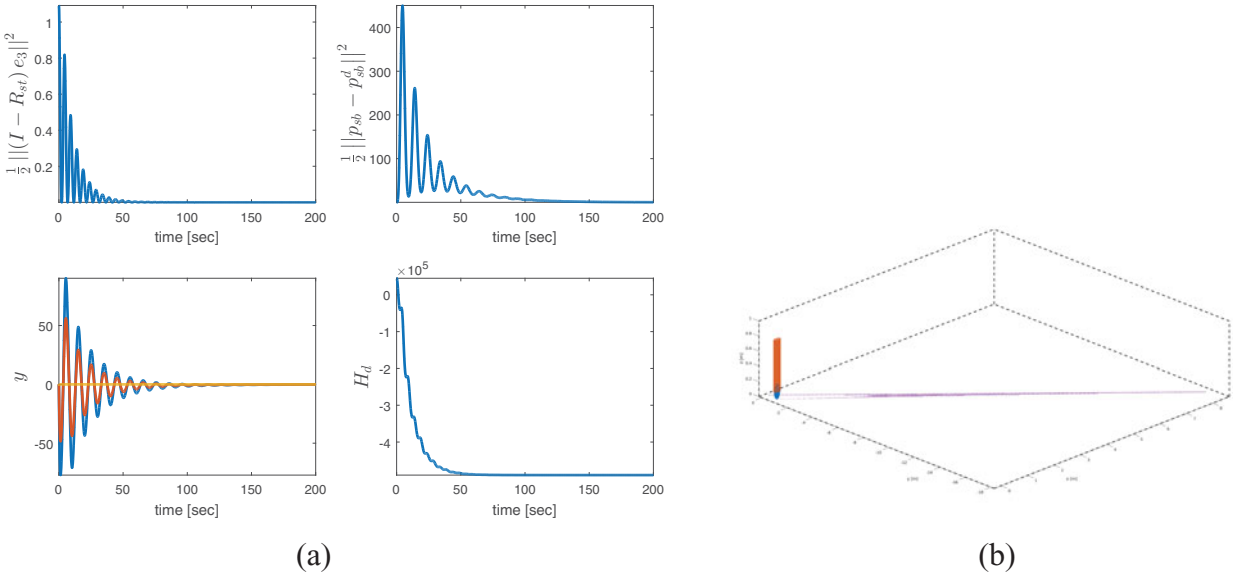

Figure 5. Asymptotic translational stabilisation of the 3D ballbot. (a) Time evolution of quantities of interest, (b) the path tracked by the ballbot.

equilibrium $R_{st} = e^{\rho \hat{e}_3}$ and the desired ball orientation $R_{sb} = e^{\sigma \hat{e}_3}$, where ρ and σ are constant real numbers. Figure 4(a) illustrates the asymptotic stabilisation. The top two plots illustrate the fact that both the ball and the top moves to an orientation such that $R_{st}e_3 = e_3$ and $R_{sb}e_3 = e_3$, which is another way to state that $R_{st} = e^{\rho \hat{e}_3}$ and $R_{sb} = e^{\sigma \hat{e}_3}$ for some constant numbers ρ and σ. The bottom left plot shows the evolution of the passive output $y = k_1 y_1 + k_2 y_2$, while the bottom right plot shows the evolution of the closed-loop energy functional H_d (21). The path tracked by the ballbot on the plane is shown in Figure 4(b).

Finally, we present the simulation results that use the controller (28), designed to stabilise the position of the ball along with the upward equilibrium of the top. The initial conditions and the control gains are selected as the third row of Table 2. In Figure 5(a), the top left figure shows that the top asymptotically converges to the upward equilibrium point where $\Gamma = e_3$. The top left figure depicts the evolution of the position error of the ball which converges to zero, indicating that $p_{sb} \to p_{sb}^d$. Additionally, while the bottom left plot shows that the passive output is asymptotically driven to zero, the bottom right plot shows that the closed-loop energy function H_d converges to its minimum value, as expected due to the detectability of the passive output y. Again, the path tracked by the ballbot on the plane is shown in Figure 5(b).

5. Conclusion

A reduced set of dynamics for the ballbot system whose configuration space is $Q = \mathbb{R}^2 \times SO(3) \times SO(3)$ has been derived. These 10 first-order ODEs are able to express the motion of the system comprehensibly, given the kinematic relations that the system has to satisfy. We are able to analyse dynamic properties and derive control laws that achieve asymptotic stabilisation for a number of purposes, thanks to the compact form of these equations of motion. In particular, both for the restricted 2D dynamics and the full 3D dynamics, we have identified two passive outputs, which are then used to devise energy-shaping control laws which make the system behave as a new Lagrangian system whose desired equilibrium point is asymptotically stable. The basin of attraction has been shown to be global as long as the mechanism is designed so that it is strongly inertially coupled.

We emphasise that modelling, analysis and computations can be carried out directly in terms of a geometric coordinate-free framework as illustrated for the ballbot in this paper. This fact facilitates the analysis of the dynamics and control synthesis for complex systems such as the ballbot.

Nomenclature

δX	Variation of the quantity X taken on the appropriate manifold
ℓ	Reduced lagrangian of the ballbot expressed as a function from $\mathfrak{so}(3) \times \mathfrak{so}(3) \times \mathbb{S}^2 \times \mathbb{R}^2$ to $\mathbb{R}$
Γ	Unit vector from the CoM of the ball to the CoM of the top expressed in the inertial frame $[m]$
ω_{ab}	Angular velocity of frame b with respect to frame a $[rad \cdot s^{-1}]$
τ	Control input actuating the relative orientation of the top with respect to the ball $[N \cdot m]$
Ad	Adjoint mapping on the Lie group $SO(3)$
g	Gravitational acceleration $[m \cdot s^{-2}]$
g_{ab}	Homogeneous transformation of frame b with respect to frame a
H_d	Desired Hamiltonian function
H_i	Storage function corresponding to the passive output y_i
I_3	The three-dimensional identity matrix
I_a	Inertia matrix (rotational) of body a, expressed in the inertial frame $[kg \cdot m^2]$
K_a	Kinetic energy of body a expressed with respect to the inertial frame $[J]$
K_k, K_I, k_a, k_i	(Matrices of) control gains
L	Lagrangian of the ballbot expressed as a function from the tangent bundle TQ to $\mathbb{R}$
l	Distance from the CoM of the ball to the CoM of the top $[m]$
m_a	Mass matrix of body a, expressed in the inertial frame $[kg]$
M_d	Desired mass matrix
p_{ab}	Position vector from the origin of frame a to the origin of frame b $[m]$
r	Radius of the ball $[m]$
R_{ab}	Rotation matrix of frame b with respect to frame a
V_a	Potential energy of body a expressed with respect to the inertial frame $[J]$
V_d	Desired potential function
V_{ab}	Twist of frame b with respect to frame a
v_{ab}	Linear velocity of frame b with respect to frame a $[m \cdot s^{-1}]$

y_i Passive output function identified after partial feedback linearization

Acknowledgment

This work was supported by the RoDyMan project, which has received funding from the European Research Council FP7 under Advanced Grant 320992.

Disclosure statement

No potential conflict of interest was reported by the authors.

Funding

European Research Council [FP7-320992].

References

Asgari, P., Zarafshan, P., & Moosavian, S.A.A. (2015). Manipulation control of an armed Ballbot with stabilizer. *Proceedings of the Institution of Mechanical Engineers, Part I: Journal of Systems and Control Engineering*. doi: 10.1177/0959651814567746.

Baillieul, J., Bloch, A., Crouch, P., & Marsden, J. (2008). *Nonholonomic mechanics and control*. New York, NY: Springer.

Donaire, A., Mehra, R., Ortega, R., Satpute, S., Romero, J.G., Kazi, F., & Singh, N.M. (2016). Shaping the energy of mechanical systems without solving partial differential equations. *IEEE Transactions on Automatic Control*, *61*(4), 1051–1056.

Hertig, L., Schindler, D., Bloesch, M., Remy, C., & Siegwart, R. (2013, May). Unified state estimation for a ballbot. In *2013 IEEE international conference on robotics and automation (ICRA)* (pp. 2471–2476). Karlsruhe, Germany: IEEE.

Inal, A., Morgul, O., & Saranli, U. (2012, October). A 3D dynamic model of a spherical wheeled self-balancing robot. In *2012 IEEE/RSJ international conference on intelligent robots and systems (IROS)* (pp. 5381–5386). Vilamoura, Portugal: IEEE.

Kumaga, M., & Ochiai, T. (2009, May). Development of a robot balanced on a ball: Application of passive motion to transport. In *ICRA'09. IEEE international conference on robotics and automation, 2009* (pp. 4106–4111). Kobe, Japan: IEEE.

Larimi, S.R., Zarafshan, P., & Moosavian, S.A.A. (2015). A new stabilization algorithm for a two-wheeled mobile robot aided by reaction wheel. *Journal of Dynamic Systems, Measurement, and Control*, *137*(1), 011009.

Lauwers, T., Kantor, G., & Hollis, R. (2007). One is enough! In Robotics Research, (pp. 327–336). Berlin-Heidelberg: Springer.

Lauwers, T., Kantor, G.A., & Hollis, R.L. (2006). A dynamically stable single-wheeled mobile robot with inverse mouse-ball drive. In *Proceedings IEEE international conference on robotics and automation. ICRA 2006*, (pp. 2884–2889). Orlando, FL:IEEE.

Leutenegger, S., & Fankhauser, P. (2010). *Modeling and control of a Ballbot* (Bachelor thesis). Zurich: ETH Zurich.

Lewis, A.D., & Murray, R.M. (1995). Variational principles for constrained systems: Theory and experiment. *International Journal of Non-Linear Mechanics*, *30*(6), 793–815.

Liao, C.W., Tsai, C.C., Li, Y.Y., & Chan, C.K. (2008, August). Dynamic modeling and sliding-mode control of a Ball robot with inverse mouse-ball drive. In *SICE annual conference, 2008* (pp. 2951–2955). Fukuoka, Japan: IEEE.

Murray, R.M., Sastry, S.S., & Zexiang, L. (1994). *A mathematical introduction to robotic manipulation* (1st ed.). Boca Raton, FL: CRC Press.

Nagarajan, U., Kantor, G., & Hollis, R. (2012, May). Integrated planning and control for graceful navigation of shape-accelerated underactuated balancing mobile robots. In *IEEE international conference on robotics and automation (ICRA)*, (pp. 136–141). St. Paul, MN: IEEE.

Nagarajan, U., Kantor, G., & Hollis, R. (2013). The ballbot: An omnidirectional balancing mobile robot. *International Journal of Robotics Research*, *33*(6), 917–930.

Nagarajan, U., Kim, B., & Hollis, R. (2012, May). Planning in high-dimensional shape space for a single-wheeled balancing mobile robot with arms. In *IEEE international conference on robotics and automation (ICRA)*, (pp. 130–135). St. Paul, MN: IEEE.

Nagarajan, U., Mampetta, A., Kantor, G.A., & Hollis, R.L. (2009, May). State transition, balancing, station keeping, and yaw control for a dynamically stable single spherical wheel mobile robot. In *IEEE International conference on robotics and automation (ICRA)* (pp. 998–1003). Kobe, Japan: IEEE.

Nguyen, H.G., Morrell, J., Mullens, K.D., Burmeister, A.B., Miles, S., Farrington, N., … Gage, D.W. (2004). Segway robotic mobility platform. In *Optics East* (pp. 207–220). SPIE, International Society for Optics and Photonics.

Satici, A.C., Ruggiero, F., Lippiello, V., & Siciliano, B. (2016, July). Intrinsic Euler–Lagrange dynamics and control analysis of the ballbot. In *2016 American control conference (ACC)* (pp. 5685–5690). Boston, MA: IEEE.

Schneider, D. (2002). Non-holonomic Euler–Poincaré equations and stability in Chaplygin's sphere. *Dynamical Systems: An International Journal*, *17*(2), 87–130.

Spong, M. (1994, Sep). Partial feedback linearization of underactuated mechanical systems. In *Proceedings of the IEEE/RSJ/GI international conference on intelligent robots and systems'94. 'Advanced Robotic Systems and the Real World', IROS'94* (Vol. 1, pp. 314–321). Munich, Germany: IEEE.